

Making Split Learning Resilient to Label Leakage by Potential Energy Loss

Fei Zheng¹, Chaochao Chen¹, Binhui Yao², Xiaolin Zheng^{1*}

¹Zhejiang University, ² Midea

{zfscgy2,zjuccc,xlzheng}@zju.edu.cn, tony.yao@midea.com

Abstract

As a practical privacy-preserving learning method, split learning has drawn much attention in academia and industry. However, its security is constantly being questioned since the intermediate results are shared during training and inference. In this paper, we focus on the privacy leakage problem caused by the trained split model, i.e., the attacker can use a few labeled samples to fine-tune the bottom model, and gets quite good performance. To prevent such kind of privacy leakage, we propose the potential energy loss to make the output of the bottom model become a more ‘complicated’ distribution, by pushing outputs of the same class towards the decision boundary. Therefore, the adversary suffers a large generalization error when fine-tuning the bottom model with only a few leaked labeled samples. Experiment results show that our method significantly lowers the attacker’s fine-tuning accuracy, making the split model more resilient to label leakage.

1 Introduction

Split learning (Vepakomma et al. 2018; Gupta and Raskar 2018) is a practical method for privacy-preserving machine learning on distributed data. By splitting the model into multiple parts (sub-models), split learning allows different parties to keep their data locally and only to share the intermediate output of their sub-models. Compared to cryptographic methods like (Mohassel and Zhang 2017; Rathee et al. 2020; Zhicong et al. 2022), split learning is much more efficient in computation and communication. To date, split learning have been applied in multiple fields, e.g., multi-task learning (Kim et al. 2020), medical research (Ha et al. 2021), and the internet of things (Koda et al. 2020).

To perform split learning, the model should be split into multiple parts. Without loss of generality, we suppose the model is split into two parts, i.e., the bottom model M_b and the top model M_t , held by the feature owner (referred as Alice) and the label owner (referred as Bob), respectively. As shown in Figure 1 (top part), during the forward pass, Alice feeds the input feature X to the bottom model to get the intermediate output $O_b = M_b(X)$, then sends O_b to Bob. Bob feeds O_b to the top model and gets the prediction $\hat{Y} = M_t(O_b)$. As for the backward pass, Bob computes the gradients on the loss $\partial L / \partial M_t$ and $\partial L / \partial O_b$. He uses the

former one to update M_t and sends the latter one to Alice. Alice then computes the gradient with regard to M_b and updates its parameters. From the above description, we can see that split learning is very straightforward with probably optimal computation and communication overhead.

However, the price for efficiency is privacy. Many previous studies have investigated the privacy leakage of input features in split learning caused by the *exchange of intermediate results* (Abuadbba et al. 2020; Pasquini, Ateniese, and Bernaschi 2021). Instead, we focus on the privacy leakage caused by the *trained split model itself* in classification tasks, which has been demonstrated by (Fu et al. 2022a). Consider the two-party split learning scenario described in the previous paragraph. As shown in Figure 1 (bottom part), if M_b is trained well, it gains the ability to separate samples of different classes and cluster the samples of the same class, in other words, O_b becomes ‘meaningful’ and highly correlated with the label. Hence, with a few leaked labeled samples, Alice (or whoever obtains the bottom model) may be able to fine-tune M_b with a random initialized M_t and then obtain a high-performance classification model. In this case, Alice not only ‘steals’ the complete model, but also obtains the label of the training samples. Considering that the complete model shall be a common property of Alice and Bob, and the label is a private asset of Bob, such *fine-tuning attack* caused by *label leakage* poses a significant privacy risk on split learning.

Protection of input features in split learning is already studied. For example, Vepakomma et al. (2020) decorrelates O_b and X by adding distance correlation (Székely, Rizzo, and Bakirov 2007) loss. This method is empirically successful because O_b does not need to contain the majority of X ’s information—it only needs to contain the part most relevant to the label Y . On the other side, protecting label information is more challenging. Since $M_t(O_b) = \hat{Y}$ is the model prediction, O_b contains all information about \hat{Y} . While the training target is to make the prediction \hat{Y} and the real label Y as close as possible, it seems impossible to prevent the attacker from deriving Y from O_b .

To solve this problem, in this paper, we view it from a different perspective. At first glance, the attacker’s target seems exactly the same as Bob’s training objective, i.e., to learn a mapping from O_b to Y . But there is a crucial difference

*Corresponding author

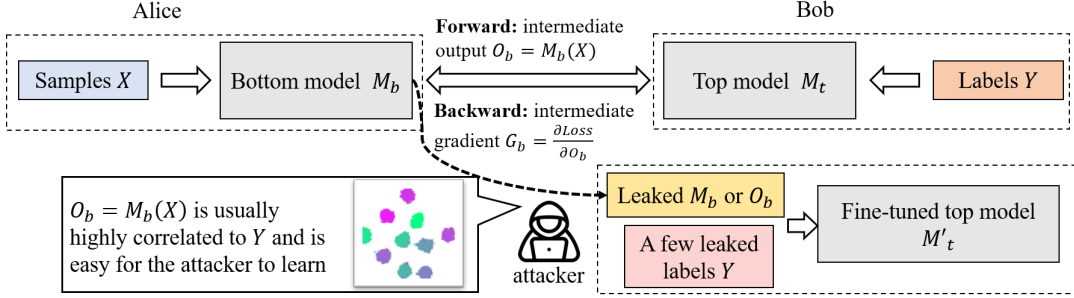


Figure 1: Label leakage attack of split learning.

between them. Alice and Bob perform the learning procedure on the entire training dataset, but on the contrary, the attacker can only access a small number of labeled samples by assumption. The problem now turns into modifying O_b 's distribution so that the attacker generalizes poorly with a few labeled samples while the benign learner has a low generalization error with sufficient labeled samples. We observe that such distribution can be obtained if the data points of the same class are distributed near the boundary of the decision region. However, during vanilla split learning, the bottom model outputs of different classes tend to separate from each other while the outputs of the same class are densely clustered, which is opposite to our purpose.

A well-known phenomenon in physics is the electrostatic equilibrium, i.e., all the net charges distribute on the surface of the conductor. Interestingly, this distribution happens to be the desired distribution for O_b , if we consider the charges as the outputs of the same class. One reason for this phenomenon is that there is a repulsive force between any pairs of like charges (charges that have the same sign, e.g., positive charges). Inspired by this, we propose the *potential energy loss* on the output of the bottom model. The potential energy loss adds a repulsive force between each pair of same-class outputs of the bottom model. During training, same-class outputs are pushed towards the boundary of the decision region, resulting in a large generalization error for the adversary. Hence, the adversary cannot fine-tune the bottom model to good performance with a small number of leaked labeled samples. In total, we make the following main contributions:

- We formalize the privacy leakage of the bottom model in terms of the generalization error of the attacker and demonstrate that making data points lie near the decision boundary helps to protect privacy.
- We propose the potential energy loss on the outputs of the bottom model to push them to their decision boundary.
- We conduct experiments on multiple datasets, showing that our method significantly reduces the attacker's fine-tuning accuracy under a small number of leaked labels.

2 Related work

2.1 Privacy concerns of split learning

Many studies have demonstrated the privacy concerns of split learning. Most of them focus on the privacy of input features.

Abuadba et al. (2020) shows that applying split learning to CNN models can be dangerous since the intermediate output is highly correlated to the input. Pasquini, Ateniese, and Bernaschi (2021); Luo et al. (2021) propose methods for feature inference attack of split learning under certain conditions. As for the privacy of the label data, Li et al. (2021) investigated the label leakage brought by the backward gradients from the top model and has proposed a solution based on a random perturbation method. Fu et al. (2022a) pointed out that besides the gradients, the trained bottom model can be easily fine-tuned with just a few labeled samples, hence the label of the training data can be inferred.

2.2 Privacy protection for split learning

One straightforward way to protect privacy for split learning is to use cryptographic privacy-preserving machine learning systems, e.g., (Mohassel and Zhang 2017; Rathee et al. 2020; Zhicong et al. 2022). Those methods utilize cryptographic building blocks to realize secure training and inference of machine learning models. However, cryptographic methods have heavy computation and communication costs and yet are not practical in many scenarios. There are also hybrid methods like (Fu et al. 2022b; Zhou et al. 2022) that only use cryptographic algorithms in some parts of the split model to balance privacy and efficiency. As for non-cryptographic methods, Vepakomma et al. (2020) adds a distance correlation (Szekely, Rizzo, and Bakirov 2007) loss to decorrelate the output of the bottom model and the input features. Li et al. (2021) protects the label information from backward gradients via perturbation.

2.3 Data-dependent generalization error

Most studies on the data-dependent generalization error are based on the Rademacher and Gaussian complexity (Koltchinskii and Panchenko 2002; Kontorovich and Weiss 2014; Lei et al. 2019), or the mutual information between the data and the algorithm output (Negrea et al. 2019; Pensia, Jog, and Loh 2018; Russo and Zou 2020). Although these studies relate the generalization bound to the data, they usually use the training data to estimate values such as complexities or information metrics, instead of directly using the data distribution. Recently, Jin et al. (2020) derived generalization bounds directly from the data distribution, by proposing the so-called cover complexity, which is a metric to measure the

‘complexity’ of the multi-class data distribution, and is computed from the distances between same-class data points and different-class data points. It is somewhat related to our work since our method makes the data distribution more ‘complicated’ by pushing the data points to the decision boundary of their class.

3 Problem

In this section, we demonstrate and formalize the privacy problem arising from the bottom model output in split learning.

3.1 Leakage from bottom model output

The output of the bottom model is the hidden representation of a certain layer in the neural network. The hidden representations of neural networks are widely studied (Rauber et al. 2017; Pezzotti et al. 2018; Cantareira, Etemad, and Paulovich 2020). Through visualization and other techniques, those studies show that the neural network gradually learns to make hidden representations of different classes separate, and those of the same class close to each other. Although this ‘separation ability’ seems to be essential for neural networks and may be the reason why they perform well on various tasks, it also brings security hazards for split learning. With only a few labeled samples and the bottom model, the attacker can fine-tune the model and obtain quite good performance. He may also use the fine-tuned model to predict the label of all the training samples with high accuracy. Hence, both the entire model and the label of the training set could be stolen by the attacker.

3.2 Threat model

We assume that the attacker has access to the trained bottom model M_b , along with a few labeled samples X'_k, Y'_k which include k samples for each class. The attacker also knows the architecture of the top model M_t , and performs the fine-tuning attack via training M_t , given X'_k and Y'_k , with pre-trained M_b fixed.

Notably, we do not consider the privacy leakage of the training procedure, during which the attacker may infer the label from the backward gradients. To prevent leakage from backward gradients, existing approaches like cryptographic methods and perturbation on the gradients can be used. Readers can refer to Section 2.2 for details.

3.3 Problem formulation

In order to reduce the aforementioned privacy leakage while maintaining the model performance at the same time, our purpose is to train a split model $M = (M_b, M_t)$ such that M_b is hard to fine-tune, while M still has a high performance. To be specific, we define the fine-tuning advantage as follows:

$$A_m(M_b) = \max \left\{ \mathbb{E}_{X'_k, Y'_k} \left(R[M^{(X'_k, Y'_k)}] - R[(M_b, M_t^{(M_b(X'_k), Y'_k)})] \right), 0 \right\}, \quad (1)$$

where X'_k, Y'_k is the leaked labeled data that has k instances independently drawn from each class, M_b is the given bottom model trained on the entire training set, $M_t^{(M_b(X'_k), Y'_k)}$ is the top model trained on the M_b ’s output $M_b(X'_k)$ and label Y'_k , $M^{(X'_k, Y'_k)}$ is the entire model trained on X'_k, Y'_k from scratch, and $R[\cdot]$ means the generalization error. If fine-tuning M_t results in a worse performance than training the whole model from scratch, the fine-tuning advantage is 0. We denote this situation as *perfect protection*, since that the attacker can just use leaked labels to train a better model from scratch, without using the bottom model. Hence, the fine-tuning advantage is always positive. We want to train a split model (M_b, M_t) such that:

- the performance gap between the trained split model and the split model obtained by vanilla split training $R[(M_b, M_t)] - R[(M_b^*, M_t^*)]$ is as small as possible.
- the fine-tuning advantage under a small size of leaked labeled samples is as small as possible.

4 Method: potential energy loss

In this section, we view the privacy leakage of the bottom model as a generalization problem for the attacker. By a simplified example, we show that making data points distributed near the decision boundary can increase the generalization error. Inspired by the electrostatic equilibrium and Coulomb’s law, we propose the potential energy loss on the outputs of the bottom model, to realize such distribution.

4.1 Generalization error from sampling error

Recall that our goal is to train a split model (M_b, M_t) , such that the bottom model M_b is hard to fine-tune under a small number of training samples. To decrease the attacker’s fine-tuning advantage is equivalent to increase

$\mathbb{E}_{X'_k, Y'_k} R[(M_b, M_t^{(M_b(X'_k), Y'_k)})]$. Since M_b is fixed, it can be

rewritten as $\mathbb{E}_{H'_k = M_b(X'_k), Y'_k} R[M_t^{(H'_k, Y'_k)}]$. Hence, our target becomes finding a M_b whose output distribution $M_b(X)$ satisfies: the generalization error is large when the sample size is small, and the generalization error is small when the sample size is sufficiently large.

To simplify our target, we assume that the bottom model M_b is powerful enough to output any desired distribution. Then the problem becomes finding a data distribution that introduces a large generalization error for the learner (when the sample size is small). By intuition, such data distribution should be kind of ‘complicated’ so that a small-sized sample can not represent the true distribution. However, there are also some restrictions on the output distribution so that the classification is feasible. For example, suppose the top model is a linear classifier, then the positive and negative samples should be separated by a hyperplane.

We use a simplified example to get some insights into the relationship between the data distribution and generalization error. Assume that all data points are distributed on the d -dimensional hypersphere $\{\mathbf{x} : \sum_{i=1}^d x_i^2 = 1\}$. Let the hypothe-

sis set be $\mathcal{H} = \{h : h(\mathbf{x}) = I[\mathbf{w} \cdot \mathbf{x} > t], \|\mathbf{w}\|_2 = 1\}$, where $I[\cdot]$ is the indicator function, and t is a constant threshold. We make the following assumptions:

- The probability density of positive samples only depends on $\mathbf{x} \cdot \mathbf{w}$, i.e., it is isotropic in any directions orthogonal to \mathbf{w} .
- Given a set of positive samples $S = \{\mathbf{x}_1, \dots, \mathbf{x}_n\}$, the learning algorithm simply outputs the normalized mean of these samples as the parameter of learned hypothesis, i.e., $f^{(S)}(\mathbf{x}) = I\left[\sum_{i=1}^n \mathbf{x}_i \cdot \mathbf{x} / \|\sum_{i=1}^n \mathbf{x}_i\|_2 > t\right]$.

Without loss of generality, let the target hypothesis be $f(x) = I[\mathbf{e}_1 \cdot \mathbf{x} > t]$, where $\mathbf{e}_1 = [1, 0, \dots, 0]$ is the unit vector along the first axis. Now we want to estimate the generalization error when the learned parameter $\mathbf{w} = \sum_{i=1}^n \mathbf{x}_i / \|\sum_{i=1}^n \mathbf{x}_i\|_2$ slightly differs from the true parameter \mathbf{e}_1 . Since the distribution is isotropic except in the direction of \mathbf{e}_1 , we may assume that \mathbf{w} lies on the plane expanded by the first two axis, i.e., $\mathbf{w} = \mathbf{e}_1 \cos \epsilon + \mathbf{e}_2 \sin \epsilon$, where ϵ is a small angle between \mathbf{w} and \mathbf{e}_1 . The generalization error is

$$\begin{aligned} R[\mathbf{w}] &= \mathbb{E}_{\mathbf{x} \sim S} I[x_1 > t] \cdot I[x_1 \cos \epsilon + x_2 \sin \epsilon \leq t] \\ &= \int_{\substack{x_1 > t \\ x_1 \cos \epsilon + x_2 \sin \epsilon \leq t \\ x_1^2 + \dots + x_d^2 = 1}} p(x_1, x_2, \dots, x_d) dV \\ &\leq \int_{\substack{x_1^2 + \dots + x_d^2 = 1 \\ t < x_1 \leq \frac{t}{\cos \epsilon} + \sqrt{1-t^2} \tan \epsilon}} p(x_1, x_2, \dots, x_d) dV \quad (2) \\ &\approx \int_{x_1=t}^{t+\epsilon\sqrt{1-t^2}} p_1(x_1) dx_1 \approx \epsilon p_1(t) \sqrt{1-t^2}, \end{aligned}$$

where p_1 is the marginal density function of x_1 . From (2) we can see that with ϵ fixed, the generalization bound is approximately proportional to the probability mass of the data points falling near the boundary of the target region.

In the above analysis, the estimation error ϵ is fixed. We now explore the relationship between the data distribution and the distribution of ϵ . Notice that for any random variable X , if X_1, \dots, X_m are m independent samples, we have $\mathbb{E}\left[\left(\frac{1}{m} \sum_{i=1}^m X_i - \mathbb{E}[X]\right)^2\right] = \frac{1}{m} \mathbb{E}[(X - \mathbb{E}X)^2]$. In other words, if the random variable is likely to fall far from the mean of its distribution, the sample mean tends to have a larger error. Although ϵ is not exactly the error of the sample mean in our case, it is also reasonable to assume $\mathbb{E}[\epsilon^2] \propto \mathbb{E}[(X - \mathbb{E}X)^2]$. To make (the magnitude of) ϵ larger, the data points should be away from their mean as much as possible. Interestingly, in our case, this is also equivalent to letting the data points lie near the boundary.

We show a simple illustration of the above analysis in Figure 2. The target hypothesis is the solid circle, and the learned hypothesis is the dashed circle. In the left figure, the dark blue points are three samples picked from all data points. Based on those samples, the learner makes an estimation represented by the dashed circle. As we can see in the right figure, although the estimation seems to be close to the target

hypothesis, there are still many misclassified data points (colored red). In other words, the generalization error is large. In summary, pushing data points to the boundary of the decision region will increase the generalization error for the following two reasons:

- The sampling error tends to be larger.
- A small error on the decision region will result in a large generalization error.

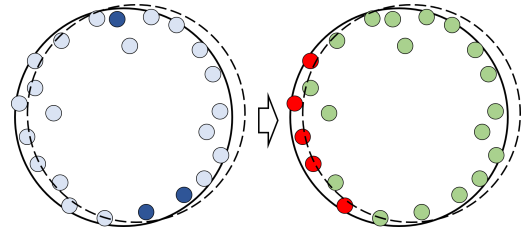


Figure 2: A small error on the decision region caused by small sample size (left) leads to a large generalization error (right).

4.2 Potential energy loss

When electrostatic equilibrium is established, any net charge resides on the surface of the conductor (Griffiths 2005, ch. 2). This is partly caused by Coulomb's law, which tells us that *like charges* (electric charges of the same sign) attract each other and *opposite charges* repel each other. Inspired by this, we can view the data points of the same class as like charges and have repulsive forces against each other. As a result, those data points will tend to be away from each other and be pushed to the boundary of the decision region.

Coulomb's law is stated as follows:

$$\mathbf{F} = k \frac{q_1 q_2 (\mathbf{r}_1 - \mathbf{r}_2)}{|\mathbf{r}_1 - \mathbf{r}_2|^3}, \quad (3)$$

where k is a constant, q_1, q_2 is the signed magnitude of the charges, $\mathbf{r}_1, \mathbf{r}_2$ are their positions, and \mathbf{F} is the repulsive force. Since we assume all data points belonging to the same class have the same sign and magnitude while ignoring the constant term, (3) becomes $\mathbf{F} = \frac{\mathbf{r}_1 - \mathbf{r}_2}{|\mathbf{r}_1 - \mathbf{r}_2|^3}$. Notice that the repulsive force is the gradient of the electric potential energy, we can further write \mathbf{F} as $\mathbf{F} = \nabla_{\mathbf{r}_1} \frac{1}{|\mathbf{r}_1 - \mathbf{r}_2|}$, which is naturally suited to the gradient descent method. Based on this, we define the *potential energy loss* (PELoss) as

$$L_{pe} = \sum_{c \in \mathcal{C}} \sum_{\mathbf{h} \in H_c} \sum_{\mathbf{h}' \in H_c, \mathbf{h}' \neq \mathbf{h}} \frac{1}{|\mathbf{h} - \mathbf{h}'|}, \quad (4)$$

where \mathcal{C} is the label set, and H_c is the bottom model outputs of c -labeled samples.

By adding L_{pe} to the loss function, during the training of the split model, the bottom model outputs of the same class are pushed away from each other, and move towards the boundary of the decision region of the top model.

Adding Layer Normalization. However, if we do not put any restrictions on \mathbf{h} , i.e., $\mathbf{h} \in \mathbb{R}^d$, the repulsive force may just push data points to somewhere far from the origin, instead of the boundary of the decision region. To overcome this, we simply enforce layer normalization (Ba, Kiros, and Hinton 2016) on \mathbf{h} , which restricts \mathbf{h} to the d -sphere of radius \sqrt{d} , i.e., $\|\mathbf{h}\|^2 = d$. Note that because the data points are on the d -sphere, the direction of repulsive force shall also be along the d -sphere. For two points \mathbf{h}, \mathbf{h}' on a d -sphere, there are two geodesics between them. Their lengths are $\arccos\langle \mathbf{h}, \mathbf{h}' \rangle$ and $2\pi - \arccos\langle \mathbf{h}, \mathbf{h}' \rangle$. So there are also two repulsive forces. When one point is at exactly the opposite position of another, i.e., their distance becomes maximum, the two repulsive forces are canceled out since the two geodesics have the same length. This is preferable since we do not want any repulsive force when two data points are already at the largest distance.

Accordingly, the potential energy loss defined in (4) should be changed to

$$L_{pe} = \sum_{c \in \mathcal{C}} \sum_{\substack{\mathbf{h}, \mathbf{h}' \in H_c \\ \mathbf{h}' \neq \mathbf{h}}} \frac{1}{\arccos\langle \mathbf{h}, \mathbf{h}' \rangle} - \frac{1}{2\pi - \arccos\langle \mathbf{h}, \mathbf{h}' \rangle}. \quad (5)$$

The combined loss for split training is $L' = L + \alpha L_{pe}$, where L is the original loss function (i.e., cross-entropy loss), α is a coefficient to control the intensity of repulsive force.

4.3 Relationship with distance correlation

Vepakomma et al. (2020) uses distance correlation as a loss to decorrelate the bottom model output and the input features. Instead, we consider the case that distance correlation loss is applied to the bottom model output and the label. The distance correlation loss on a batch is

$$L_{dcor} = \sum_{i,j=1}^n d_{i,j} d'_{i,j} / \sqrt{\sum_{i,j=1}^n d_{i,j}^2 \sum_{i,j=1}^n d'^2_{i,j}}, \quad (6)$$

where $d_{i,j}$ is the doubly-centered distance between i -th sample's output and j -th sample's output, and $d'_{i,j}$ is the doubly-centered distance between i -th label and j -th label. Assume the label is the one-hot, then the same-class samples have the same label. If the i -th sample and j -th sample belong to the same class, then $d'_{i,j} = 0$. Hence, (6) (ignoring the denominator) is converted to

$$\sum_{\substack{c, c' \in \mathcal{C} \\ c \neq c'}} \sum_{\substack{\mathbf{h} \in H_c \\ \mathbf{h}' \in H_{c'}}} k \left(|\mathbf{h} - \mathbf{h}'| - \overline{|\mathbf{h} - \cdot|} - \overline{|\cdot - \mathbf{h}'|} + \overline{|\cdot - \cdot|} \right), \quad (7)$$

where \mathcal{C} is the set of labels, k is some constant, $\overline{|\mathbf{h} - \cdot|}$ is the average distance from \mathbf{h} to other points within the batch, and $\overline{|\cdot - \cdot|}$ is the average distance between all pairs of points within the batch. We can see that minimizing the distance correlation is similar to minimizing the distance between samples of different classes. As our method is to maximize distances between same-class outputs, minimizing distance correlation has a similar effect. However, when there are multiple classes, minimizing the distance of one output to

all other classes' outputs may lead to unpredictable behaviors. For example, a certain data point is ‘attracted’ by all samples of other classes. If those other classes lie in different directions of the data point, the combined attraction could be noisy.

5 Empirical study

We conduct experiments on three different datasets, i.e., MNIST (Lecun et al. 1998), Fashion-MNIST (Xiao, Rasul, and Vollgraf 2017), and CIFAR-10 (Krizhevsky, Hinton et al. 2009), using a DNN, a convolutional network, and Resnet-20 (He et al. 2016), respectively. We compare the validation accuracy of vanilla split training, training with potential energy loss (PELoss, our method), and training with distance correlation loss (DcorLoss) proposed by (Vepakomma et al. 2020). Note that for distance correlation loss, we compute the distance correlation between the bottom model output and the label, with layer normalization added like in our method. We show the model performance vs. the attacker's fine-tuning accuracy, the convergence speed of different methods, and the visualization of bottom model outputs using t-SNE.

5.1 Experiment Settings

We describe some experiment settings below.

Implementation. All experiments are implemented using the Pytorch library¹, and are executed on a server with NVIDIA RTX3090 GPUs.

Network structures. For MNIST task, the network structure is [Linear(784, 128), LeakyReLU, Linear(128, 32), Tanh, Linear(32, 10)]. For the Fashion-MNIST task, the network structure is [Conv(1, 32, kernel_size=5), LeakyReLU, MaxPool(2), Conv(32, 64, kernel_size=3, padding=1), LeakyReLU, MaxPool(2), Linear(2304, 128), Tanh, Linear(128, 10)]. For CIFAR-10, we use the Resnet-20 structure described in the original paper (He et al. 2016).

Layer to split. The split position is a crucial factor in split learning. However, the effect of the split position varies on different model architectures. Hence, in all experiments, we split the model by its last dense layer in consistency to our analysis. The last dense layer is the top model, and all the remaining layers form the bottom model.

Training strategy. For all split training tasks, we use Adam optimizer with default parameters. For the attacker's fine-tuning tasks, since Adam performs poorly when the sample size is extremely small, we use the SGD optimizer with a learning rate of 0.01 and momentum of 0.9. The stop criterion for fine-tuning tasks is that the training error is smaller than 0.01 or the epochs reach 1,000. For training with PEloss and DcorLoss, we train the model for 100 epochs and save the best model on the validation set. We save the best model during the 90th to 100th epoch to ensure that the loss is optimized sufficiently. The attacker's accuracy is obtained by fine-tuning the saved (bottom) model. As for vanilla split training, we use the early stopping strategy of 20 epochs. We run all experiments for > 5 times and report the mean and standard error of the results.

¹<https://pytorch.org>

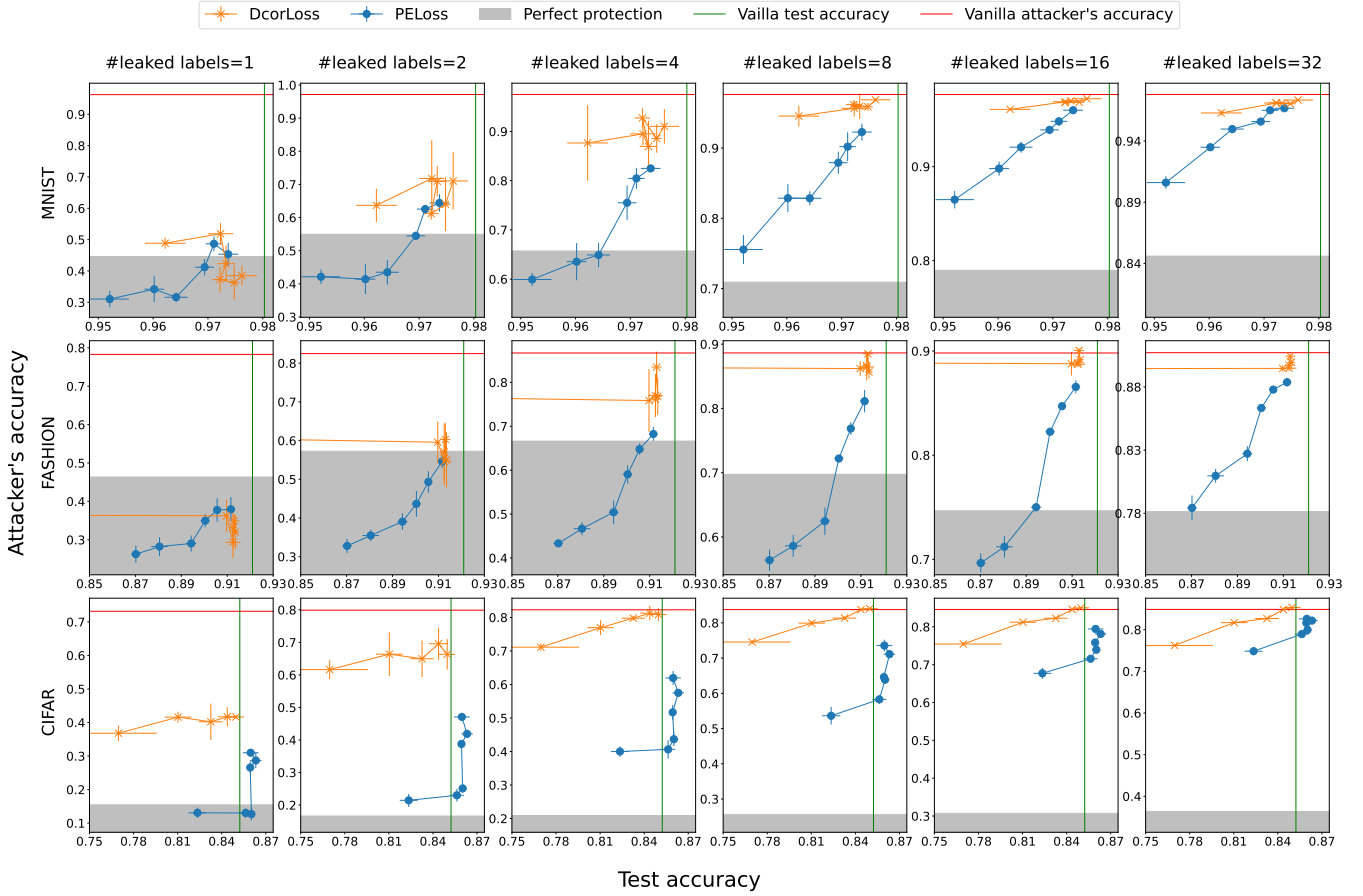


Figure 3: Test accuracy vs. attacker’s accuracy.

Data argumentation. To eliminate unnecessary variables, no data argumentation is used in our experiments, including any image flipping and random cropping. Hence, the reported model performance may be lower than those studies using data argumentation by default.

5.2 Model performance vs attacker’s accuracy

We report the test accuracy and the attacker’s accuracy obtained by both methods, with α varying from 0.5 to 16, and the number of leaked labels varying from 1 to 32, in Figure 3. For both methods, the right-upper end of the curve corresponds to the smallest α ($= 0.5$), and the left-lower end corresponds to the largest α ($= 16$). α doubles each time. We also plot the test accuracy (green line) and the attacker’s accuracy (red line) in the vanilla split learning case, and the perfect protection area (where the attacker’s accuracy is lower than the accuracy of training from scratch using leaked labels).

For both methods, we observe the trend that the increment of α decreases the attacker’s accuracy, but the test accuracy will also be lowered. Also, larger numbers of leaked labels greatly increase the attacker’s accuracy on both methods. Although both methods protect privacy at the cost of damaging the model performance, it is obvious that our proposed

PELoss is superior to DcorLoss. Our proposed PELoss has the following advantages compared with DcorLoss:

- The curve of PELoss is constantly at the lower-right side of DcorLoss. In other words, on the same test accuracy level, the PELoss has a significantly lower attacker’s accuracy than DcorLoss, indicating that PELoss has a better privacy-preserving ability.
- The curve of PELoss is smoother than the curve of DcorLoss. While the DcorLoss’s curve may randomly fluctuate as α changes, the PELoss’s curve moves lower as α increases, i.e., PELoss is more responsive to the change of α . Hence, it is easier to balance privacy and model performance using PELoss.
- When α is large enough, e.g., $\alpha = 16$, DcorLoss may make the model training diverge, while training with PELoss is more stable.

5.3 Visualization

5.4 Convergence speed

We show the convergence speed of our method in Figure 4 with $\alpha \in \{0.5, 2, 8\}$, and compare it with vanilla split training. We can see that with PELoss added, the model conver-

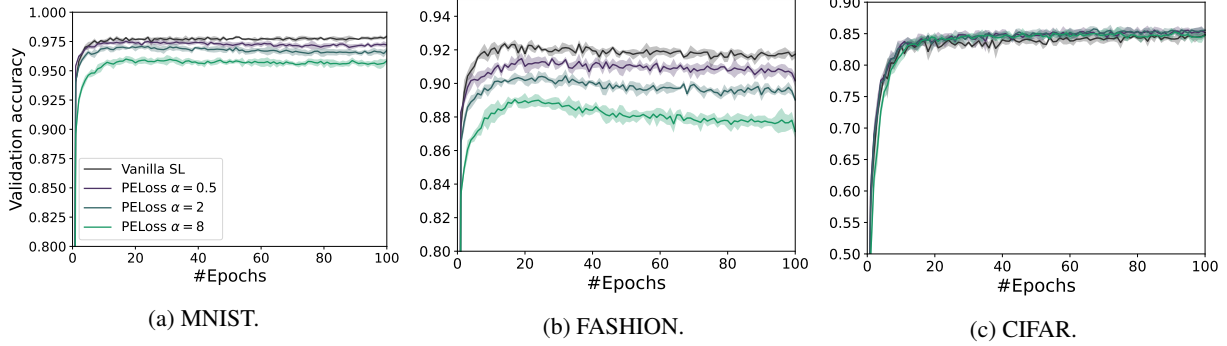


Figure 4: Convergence speed.

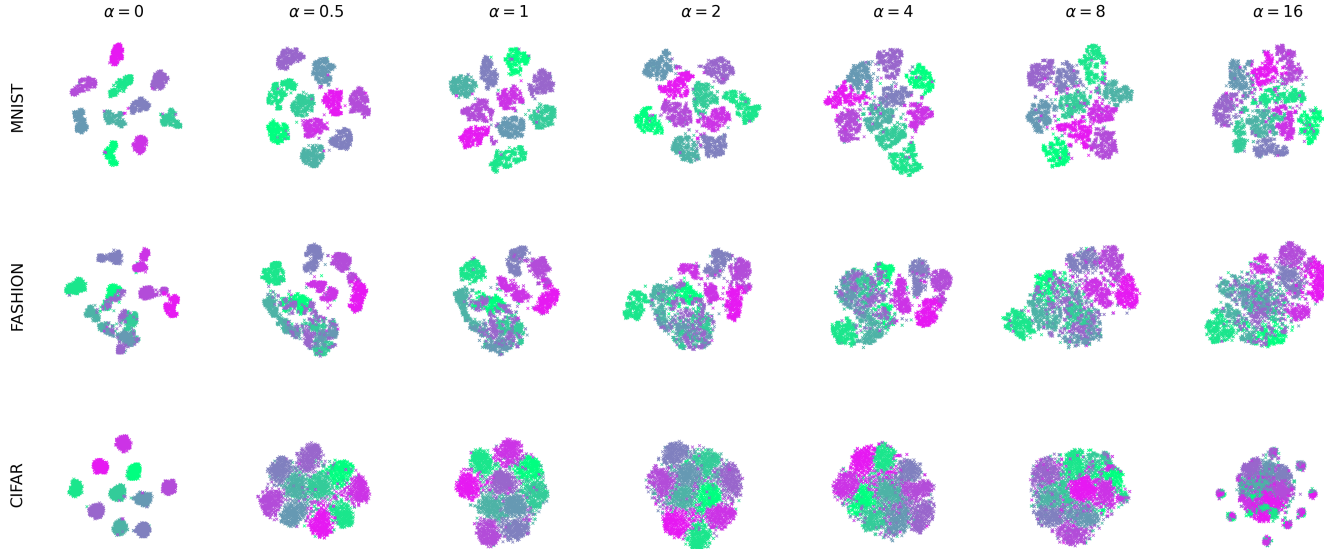


Figure 5: t-SNE of the bottom model output.

gence is slightly slowed down as α increases. However, the slowdown is nearly negligible.

We believe such a minor slowdown is acceptable in practical applications.

To directly show the effect of potential energy loss, we visualize the bottom model output using t-SNE in Figure 5. We can see that without the potential energy loss, the bottom outputs of different classes are clustered with a relatively large margin. As α increases, the clusters become fatter and even overlap with each other. We observe that the overlapping in the CIFAR-10 dataset is more obvious, possibly because the bottom model is more powerful to distort the output distribution.

6 Conclusion

In this paper, we investigate the privacy leakage of split learning arising from the learned bottom model. We view the fine-tuning attack as a learning procedure for the attacker and turn the privacy-preserving problem into a generalization maximization problem. We find that pushing data points to

their decision boundary increases the generalization error for the attacker, and propose the potential energy loss on the bottom model output. By this, we make the output of the bottom model more complicated and hard to fine-tune. Extensive experiments show that our method significantly restricts the ability of the attacker's fine-tuning attack, with only a minor decrease in model performance. Compared with the existing approach of using distance correlation loss, our method is more effective and stable.

There are also some limitations of our work. First, we assume that the attacker is using a supervised learning approach to fine-tune the bottom model, ignoring that the attacker may also obtain all those unlabeled bottom model outputs and conduct some attacks based on non-supervised learning approaches, e.g., clustering. Second, more studies on different model architectures, split positions, and tasks are needed.

References

Abuadbba, S.; Kim, K.; Kim, M.; Thapa, C.; Çamtepe, S. A.; Gao, Y.; Kim, H.; and Nepal, S. 2020. Can We Use Split

Learning on 1D CNN Models for Privacy Preserving Training? In Sun, H.; Shieh, S.; Gu, G.; and Ateniese, G., eds., *ASIA CCS '20: The 15th ACM Asia Conference on Computer and Communications Security, Taipei, Taiwan, October 5-9, 2020*, 305–318. ACM.

Ba, J. L.; Kiros, J. R.; and Hinton, G. E. 2016. Layer Normalization.

Cantareira, G. D.; Etemad, E.; and Paulovich, F. V. 2020. Exploring Neural Network Hidden Layer Activity Using Vector Fields. *Inf.*, 11(9): 426.

Fu, C.; Zhang, X.; Ji, S.; Chen, J.; Wu, J.; Guo, S.; Zhou, J.; Liu, A. X.; and Wang, T. 2022a. Label inference attacks against vertical federated learning. In *31st USENIX Security Symposium (USENIX Security 22), Boston, MA*.

Fu, F.; Xue, H.; Cheng, Y.; Tao, Y.; and Cui, B. 2022b. BlindFL: Vertical Federated Machine Learning without Peeking into Your Data. In Ives, Z.; Bonifati, A.; and Abbadi, A. E., eds., *SIGMOD '22: International Conference on Management of Data, Philadelphia, PA, USA, June 12 - 17, 2022*, 1316–1330. ACM.

Griffiths, D. J. 2005. Introduction to electrodynamics.

Gupta, O.; and Raskar, R. 2018. Distributed learning of deep neural network over multiple agents. *J. Netw. Comput. Appl.*, 116: 1–8.

Ha, Y. J.; Yoo, M.; Lee, G.; Jung, S.; Choi, S. W.; Kim, J.; and Yoo, S. 2021. Spatio-Temporal Split Learning for Privacy-Preserving Medical Platforms: Case Studies With COVID-19 CT, X-Ray, and Cholesterol Data. *IEEE Access*, 9: 121046–121059.

He, K.; Zhang, X.; Ren, S.; and Sun, J. 2016. Deep Residual Learning for Image Recognition. In *2016 IEEE Conference on Computer Vision and Pattern Recognition, CVPR 2016, Las Vegas, NV, USA, June 27-30, 2016*, 770–778. IEEE Computer Society.

Jin, P.; Lu, L.; Tang, Y.; and Karniadakis, G. E. 2020. Quantifying the generalization error in deep learning in terms of data distribution and neural network smoothness. *Neural Networks*, 130: 85–99.

Kim, J.; Shin, S.; Yu, Y.; Lee, J.; and Lee, K. 2020. Multiple Classification with Split Learning. In *SMA 2020: The 9th International Conference on Smart Media and Applications, Jeju, Republic of Korea, September 17 - 19, 2020*, 358–363. ACM.

Koda, Y.; Park, J.; Bennis, M.; Yamamoto, K.; Nishio, T.; Morikura, M.; and Nakashima, K. 2020. Communication-Efficient Multimodal Split Learning for mmWave Received Power Prediction. *IEEE Communications Letters*, 24(6): 1284–1288.

Koltchinskii, V.; and Panchenko, D. 2002. Empirical margin distributions and bounding the generalization error of combined classifiers. *The Annals of Statistics*, 30(1): 1–50.

Kontorovich, A.; and Weiss, R. 2014. Maximum Margin Multiclass Nearest Neighbors. In *Proceedings of the 31th International Conference on Machine Learning, ICML 2014, Beijing, China, 21-26 June 2014*, volume 32 of *JMLR Workshop and Conference Proceedings*, 892–900. JMLR.org.

Krizhevsky, A.; Hinton, G.; et al. 2009. Learning multiple layers of features from tiny images.

Lecun, Y.; Bottou, L.; Bengio, Y.; and Haffner, P. 1998. Gradient-based learning applied to document recognition. *Proceedings of the IEEE*, 86(11): 2278–2324.

Lei, Y.; Dogan, Ü.; Zhou, D.; and Kloft, M. 2019. Data-Dependent Generalization Bounds for Multi-Class Classification. *IEEE Trans. Inf. Theory*, 65(5): 2995–3021.

Li, O.; Sun, J.; Yang, X.; Gao, W.; Zhang, H.; Xie, J.; Smith, V.; and Wang, C. 2021. Label Leakage and Protection in Two-party Split Learning. In *International Conference on Learning Representations*.

Luo, X.; Wu, Y.; Xiao, X.; and Ooi, B. C. 2021. Feature Inference Attack on Model Predictions in Vertical Federated Learning. In *37th IEEE International Conference on Data Engineering, ICDE 2021, Chania, Greece, April 19-22, 2021*, 181–192. IEEE.

Mohassel, P.; and Zhang, Y. 2017. SecureML: A System for Scalable Privacy-Preserving Machine Learning. In *2017 IEEE Symposium on Security and Privacy, SP 2017, San Jose, CA, USA, May 22-26, 2017*, 19–38. IEEE Computer Society.

Negrea, J.; Haghifam, M.; Dziugaite, G. K.; Khisti, A.; and Roy, D. M. 2019. Information-Theoretic Generalization Bounds for SGLD via Data-Dependent Estimates. In Wallach, H. M.; Larochelle, H.; Beygelzimer, A.; d'Alché-Buc, F.; Fox, E. B.; and Garnett, R., eds., *Advances in Neural Information Processing Systems 32: Annual Conference on Neural Information Processing Systems 2019, NeurIPS 2019, December 8-14, 2019, Vancouver, BC, Canada*, 11013–11023.

Pasquini, D.; Ateniese, G.; and Bernaschi, M. 2021. Unleashing the Tiger: Inference Attacks on Split Learning. In Kim, Y.; Kim, J.; Vigna, G.; and Shi, E., eds., *CCS '21: 2021 ACM SIGSAC Conference on Computer and Communications Security, Virtual Event, Republic of Korea, November 15 - 19, 2021*, 2113–2129. ACM.

Pensia, A.; Jog, V. S.; and Loh, P. 2018. Generalization Error Bounds for Noisy, Iterative Algorithms. In *2018 IEEE International Symposium on Information Theory, ISIT 2018, Vail, CO, USA, June 17-22, 2018*, 546–550. IEEE.

Pezzotti, N.; Höllt, T.; van Gemert, J. C.; Lelieveldt, B. P. F.; Eisemann, E.; and Vilanova, A. 2018. DeepEyes: Progressive Visual Analytics for Designing Deep Neural Networks. *IEEE Trans. Vis. Comput. Graph.*, 24(1): 98–108.

Rathee, D.; Rathee, M.; Kumar, N.; Chandran, N.; Gupta, D.; Rastogi, A.; and Sharma, R. 2020. CrypTFlow2: Practical 2-Party Secure Inference. In Ligatti, J.; Ou, X.; Katz, J.; and Vigna, G., eds., *CCS '20: 2020 ACM SIGSAC Conference on Computer and Communications Security, Virtual Event, USA, November 9-13, 2020*, 325–342. ACM.

Rauber, P. E.; Fadel, S. G.; Falcão, A. X.; and Telea, A. C. 2017. Visualizing the Hidden Activity of Artificial Neural Networks. *IEEE Trans. Vis. Comput. Graph.*, 23(1): 101–110.

Russo, D.; and Zou, J. 2020. How Much Does Your Data Exploration Overfit? Controlling Bias via Information Usage. *IEEE Trans. Inf. Theory*, 66(1): 302–323.

Székely, G. J.; Rizzo, M. L.; and Bakirov, N. K. 2007. Measuring and testing dependence by correlation of distances. *The Annals of Statistics*, 35(6): 2769 – 2794.

Vepakomma, P.; Gupta, O.; Swedish, T.; and Raskar, R. 2018. Split learning for health: Distributed deep learning without sharing raw patient data.

Vepakomma, P.; Singh, A.; Gupta, O.; and Raskar, R. 2020. NoPeek: Information leakage reduction to share activations in distributed deep learning. In Fatta, G. D.; Sheng, V. S.; Cuzzocrea, A.; Zaniolo, C.; and Wu, X., eds., *20th International Conference on Data Mining Workshops, ICDM Workshops 2020, Sorrento, Italy, November 17-20, 2020*, 933–942. IEEE.

Xiao, H.; Rasul, K.; and Vollgraf, R. 2017. Fashion-MNIST: a Novel Image Dataset for Benchmarking Machine Learning Algorithms.

Zhicong, H.; Wen-jie, L.; Cheng, H.; and Jiansheng, D. 2022. Cheetah: Lean and Fast Secure Two-Party Deep Neural Network Inference. In *31st USENIX Security Symposium (USENIX Security 22)*. Boston, MA: USENIX Association.

Zhou, J.; Zheng, L.; Chen, C.; Wang, Y.; Zheng, X.; Wu, B.; Chen, C.; Wang, L.; and Yin, J. 2022. Toward Scalable and Privacy-preserving Deep Neural Network via Algorithmic-Cryptographic Co-design. *ACM Transactions on Intelligent Systems and Technology (TIST)*, 13(4): 1–21.